BJET
(Bayero Journal of Engineering and Technology)
https://bjet.ng/index.php/jet

Research Article
2025, Vol. 20 (1), 8-12

EVALUATION OF GALVANIC CORROSION FAILURE OF COUPLED DISSIMILAR STEEL PIPES FOR BOREHOLE APPLICATION

Muazu Abubakar[1*], Yusuf Tijjani[1] and Yasin Shehu Bala[1]

[1] Department of Electrical Engineering, Bayero University, Kano, Nigeria.

[*]Corresponding author email: amuazu.mec@buk.edu.ng

Received: 19-05-2025
Revised: 24-05-2025
Accepted: 31-05-2025
Published: 10-06-2025

Abstract: *In this work, the corrosion failure analysis of two connected dissimilar pipes obtained from a borehole site was investigated. The chemical composition and microstructure of the pipes were obtained using XRF and optical microscopy respectively. The corrosion potential (Ecor) and corrosion current (Icor) of the two pipes were determined using the Tafel polarization curve in water obtained from the borehole. In addition, SEM and EDX of the inside and outside of the pipes were conducted. From the results, it shows that the carbon contents of the two pipes were different. Potentiodynamic polarization results revealed that Steel pipe A exhibited a more negative corrosion potential (-0.75 to -0.55 V vs SCE) and higher corrosion current compared to Steel pipe B (-0.55 to -0.35 V vs SCE), potentially leading to galvanic cell formation when coupled. The SEM and EDX further show that one of the pipes has undergone more oxidation than the other. This shows that coupling two dissimilar steel pipes for borehole application can lead to corrosion failure.*

Key words: Galvanic corrosion; steel pipe; corrosion potential; corrosion current.

1. Introduction

A galvanic cell is created when two dissimilar metals with two different electrode potentials are connected electrically in the presence of an electrolyte. In a galvanic cell, the anode is where the dissolution occurs, while the cathode is protected by the electrons supplied by the anode (Bellucci, 1991). Local plumbers are in the habit of coupling two dissimilar steel pipes during the piping of boreholes in Nigeria. However, this practice causes one of the steels to corrode faster, which leads to the failure of the piping system.

Several studies have reported the effect of the corrosion behavior of joining dissimilar steel materials and steel with other materials. For example, Zhou et al. (2021) studied the corrosion behavior of joining two dissimilar stainless steels. Open circuit potentials have been recorded for the stainless steels 304 and 420 as -0.11V vs SCE and 0.51V vs SCE respectively. The steel with -0.51V vs SCE was considered the anode due to its more negative po-tential. In another study, Shaik and Thamida (2019) studied the galvanic corrosion of tri-metallic joints of steels. The tri-metallic steels SS316, SS304 and SS202 were found to have potentials and currents of -0.0953V vs SCE/ 0.03981 µA/cm2, -0.0895V vs SCE/0.23125 µA/cm2 and -0.1140 V vs SCE/0.73989 µA/cm2 respectively. Steel SS202 was considered anodic due to its most negative corrosion potential and high corrosion current. In similar research, Ghorbani et al. (2017) studied the corrosion behavior of dissimilar ferritic and austenitic stainless-steel joints; corrosion potential and corrosion current in the range of -0.091–-0.544 V and 4.37-11.81 µA/cm2 were reported respectively. In addition, Tavak-kolizadeh and Saadat manesh (2001) reported the corrosion behavior of fiber-reinforced plastics bonded with steel. The corrosion potential and current before and after bonding were found to be -0.766 V (vs SCE)/ 3.92 µA/cm2 and -0.244V (vs SCE)/17 µA/cm2 respectively. Furthermore, Hasan (2014) studied the corrosion behavior of carbon steel in deoxygenated water and a potential of -1 V vs SCE was reported. In another work, Wu et al. (2015) studied the corrosion behavior of dissimilar joints of ferritic stainless steel and carbon steel. The corrosion potential and corrosion current of the carbon steel were found to be -0.716 V vs SCE and 152×10^{-4} mA/cm2 respectively.

The corrosion mechanisms of two dissimilar steels may be the same in the same corrosion environment;

however, their rates may be different due to differences in the chemical composition of the steels. The difference in chemical composition may prompt the formation of certain intermetallic phases, which can be anodic or cathodic to the main matrix. Normally, low-carbon steels contain pearlite in a matrix of ferrite. The ferrite phase, which is pure iron, acts as an anode during the corrosion of steel in water, while the cathodic reaction is mainly oxygen re-duction (Wu et al., 2023). The mechanism of carbon steel corrosion in water is given by the anodic and cathodic reactions as follows:

$$\mathrm{Fe} \rightarrow Fe^{2+} + 2e^{-} \quad (1)$$

$$O_2 + 2H_2O + 4e^{-} \rightarrow 4OH^{-} \quad (2)$$

The overall reaction results in the formation of Fe(OH)2 (Satoh et al., 2007). However, the Fe(OH)2 is unstable, which later oxidizes to Fe(OH)3 (Wu et al., 2023).

Some works reported the corrosion failure of carbon steel pipes due to the impact of internal pipe grooves on flow-accelerated corrosion (Bagheri et al., 2017). However, works on the effect of coupling dissimilar carbon steel pipes under a neutral corrosion environment have not been reported. The objective of this work is to characterize the failed carbon steel pipes and study their corrosion behavior in borehole water. This work does not consider the stresses set up at the junction of the thread-ed-coupled pipes.

2. Experimental

The failed steel pipes used in this study were obtained from a borehole site and the coupling is shown in Fig. 1a; the steel pipes were labeled as A and B. The section of the failed pipes was cut with a saw. The elemental chemical compositions of the coupled pipes were determined using a SPECTROMAXX metal analyzer.

Fig. 1: Steel pipes from a borehole site (a) Couple steel pipes removed from a borehole

The sections of the pipes were cut, mounted on a bakelite, polished grinded with 80-1200 grit papers with water as a lubricant. The polishing of the ground samples was conducted using 0.05µm Al2O3 powder suspension in distilled water. After the polishing operation, the etching of the polished samples was performed using nital to reveal the microstructure, and optical microscopy of the sections was recorded using OMAX.

2.1 Potentiodynamic Polarization and SEM/EDX Test

The corrosion properties using potentiodynamic polarization were performed on the steel pipes on an Electro-chemical Workstation (CS350) with a standard calomel electrode (SCE) controlled by a PC. Before the test, the steel pipe samples were cut into square shape (1mm×1mm) and then mounted on an epoxy resin. The mounted samples were then ground accordingly with various SiC grit papers in the range 80-1200 with water as a lubricant. A saturated calomel electrode (SCE) was used as the reference electrode and platinum (Pt) sheet as an auxiliary electrode and the mounted samples as a working electrode.

The potentiodynamic polarization curves of the polished surfaces of both steel pipes were determined using the corrosion current (Icorr) and voltage (Ecorr) in borehole water with a standard calomel electrode as reference electrode. SEM/EDX analyses of the inside and outside of the pipes were recorded using the JOEL-JSM 7600F machine.

3. Results and Discussion

3.1 Visual Observation

Visual observation of different sections of pipes A and B are shown in Fig. 1. Fig. 1a shows the couple of steel pipes A and B removed from a borehole. In addition, Figs. 1b and 1d show steel pipe A after the decoupling of the steel pipe, which shows corrosion attack both inside and outside of the pipe. Furthermore, steel pipe B (Fig. 1c and 1e) shows no attack at the outside of the pipe; however, the inside pipe shows evidence of corrosion attack. The corrosion attack in steel pipe A can be attributed to both uniform corrosion due to the different phases present in the steel and galvanic corrosion due to coupling with steel pipe B, while the inside corrosion of steel pipe B can be attributed to uniform corrosion of the pipe.

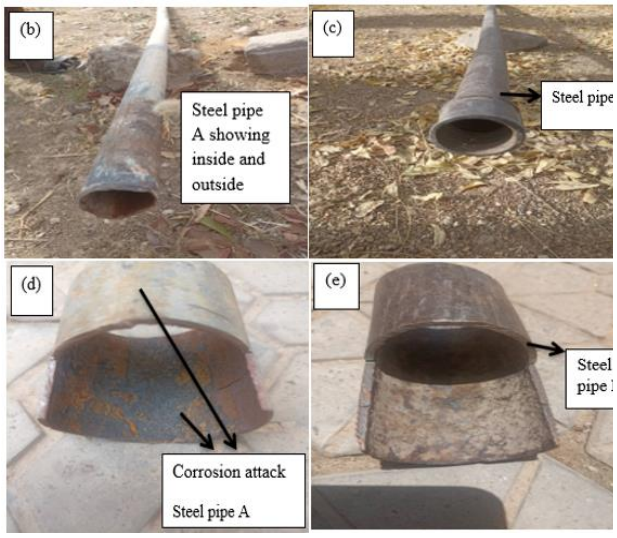

Fig. 1: Steel pipes from a borehole site (b) steel pipe A showing inside and outside corrosion (c) steel pipe B (d) section of steel pipe A with inside and outside corrosion (e) section of steel pipe B with inside corrosion

3.2 Chemical Composition of Pipes A and B

The chemical composition of the steel pipes (A and B) is shown in Table 1. From the table, the carbon content of Sample A and Sample B were found to be 0.209% and 0.107%, respectively. An increase in carbon content in steel results in an increase in mechanical properties while decreasing the corrosion resistance of steel (Pleshivtsev et al., 2009). The increase in carbon in steel resulted in the formation of cementite in the matrix of ferrite. The cementite form will be cathodic to the ferrite matrix; therefore, the more cementite, the more cathodic sites in the matrix of ferrite (Sun et al., 2014). Since the carbon content of steel A is higher than that of steel B, there is a likelihood the corrosion rate of steel A will be higher than that of B.

Table 1: Chemical composition of steel pipes A and B

Elements (%)	Steel pipe A	Steel pipe B
C	0.209	0.107
Si	0.201	0.81
Mn	1.14	0.60
P	0.012	0.030
S	0.0060	0.018
Cr	0.0026	0.0015
Mo	-	-
Ni	0.0086	0.0040
Fe	Balance	Balance

3.3 Optical Microscopy

The optical microscopy of steel pipes A and B is shown in Fig. 2. From the figure, it shows the presence of ferrite (white) and pearlite (dark) phases in both A and B. However, sample A has more pearlite than sample B. This can be attributed to the high carbon content in A. As the carbon content of steel increases, the pearlite phase, which is a lamellar structure of ferrite and cementite, increases. From Fig. 2a, it shows a large volume of dark pearlite phase. However, Fig. 2b shows a large volume of white ferrite phases in B. That means A will have less resistance to corrosion than sample B. The presence of pearlite in steels increases the susceptibility of the steel to corrosion because the pearlite causes localized corrosion in steels by acting as a cathode to ferrite (Wang et al., 2022). Apart from the galvanic effect of coupling two steels A and B, there is a likelihood of localized corrosion in steel pipes A and B due to the presence of pearlite and ferrite.

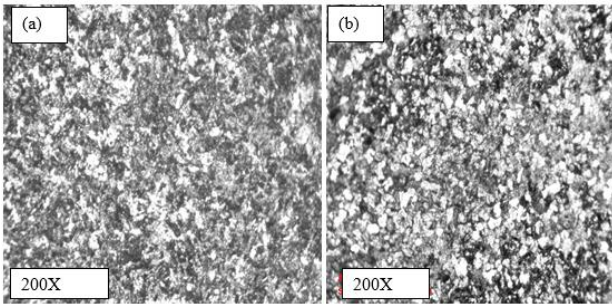

Fig. 2: Optical micrograph of (a) steel pipe A & (b) steel pipe B

3.4 Potentiodynamic Polarization of Steel Pipes A and B

The potentiodynamic polarization curves of steel pipes A and B in borehole water are shown in Fig. 3. From the figure, it shows steel pipe A has a potential (Ecorr) of -0.753 V (SCE) and steel pipe B has a potential of -0.534 V (SCE). This shows that sample A will be more susceptible to corrosion than sample B. From the thermodynamics of corrosion, ($\Delta G = -nFE$) it shows that the more negative the potential, the more the negative of ΔG, the less the resistance of the material to corrosion since n and F are constants. In addition, the corrosion currents (icorr) for steel pipes A and B were found to be 8.17×10-5 A/cm2 and 3.33×10-5 A/cm2 respectively. This shows that the corrosion rate of steel pipe A is higher than that of steel pipe B. Also, it shows that from the couple, steel pipe A will be the anode due to its more negative corrosion potential and high corrosion current, while steel pipe B will be the cathode due to its less negative potential and low corrosion current. This observation is in agreement with the chemical composition (Table 1) and the optical microscopy (Fig. 2) because the high carbon content in steel reduces its resistance to corrosion due

to the formation of more pearlite in the microstructure. Coupling the steel pipes A and B will create a galvanic cell with current flowing from pipe A to B. Therefore, B will be the cathode, and A will be the anode; hence A will be more susceptible to corrosion than B (Fig. 1b). The corrosion potential obtained for steel A agreed with Wu et al., (2015) and Tavakkolizadeh and Saadat manesh (2001).

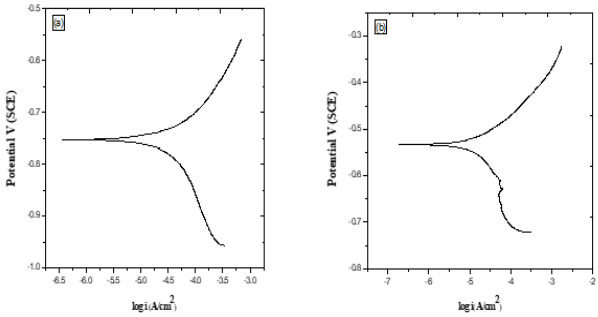

Fig. 3: Potentiodynamic polarization curves of (a) steel pipe A and (b) steel pipe B

3.5 SEM and EDX Analysis of Corroded Sections of A and B

The corroded sections of the steel pipes A and B subjected to SEM analysis and EDX are shown in Fig. 4 and Fig. 5. Fig. 4 shows SEM micrographs providing evidence of corrosion products. Steel pipe A has a higher corrosion product than steel pipe B; this is evidence that the carbon content in A makes it more susceptible to corrosion than B. In addition, the optical microstructure (Fig. 2) supports this assertion, where the microstructure of A shows more pearlitic microstructure in the ferrite matrix. The pearlitic microstructure, which is a lamellae structure of ferrite and cementite, will be a local cathode to the ferrite in steel A. Though steel B, also contains pearlite microstructure, the content is less than that of A. As a result, A will be more prone to corrosion than B, as shown in the EDX where steel pipe A has higher oxygen content than sample B. This further agrees with the result of the potentiodynamic polarization, where A has more negative potential and a high corrosion current than B. The presence of oxygen is an indication that there is an oxidation of the ferrite iron, as shown in equation 1.

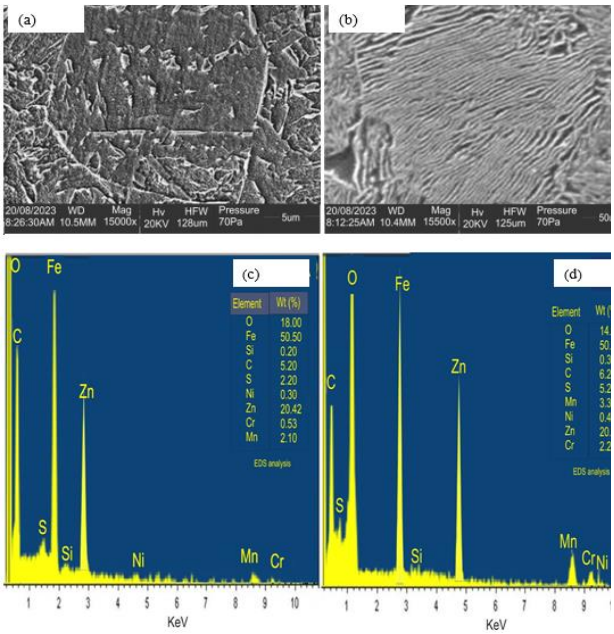

Fig. 4: SEM and EDX analysis of pipe A (a) outside corroded part (b) inside corroded part (c) EDX analysis of inside corroded part and (d) EDX analysis of outside corroded part.

However, the corrosion of sample B inside the pipe (Fig. 5) can be attributed to localized galvanic corrosion due to the different phases present in the microstructure. Localized galvanic corrosion can occur in steel samples due to the presence of ferrite and cementite in the microstructure. Normally, the ferrite in the steel sample acts as the local anode while the cementite acts as the local cathode. From the EDX results, it shows that steel pipe B has less oxygen content than steel pipe A. In addition, the more positive ECorr value of pipe B shows that it will be cathodic to pipe A.

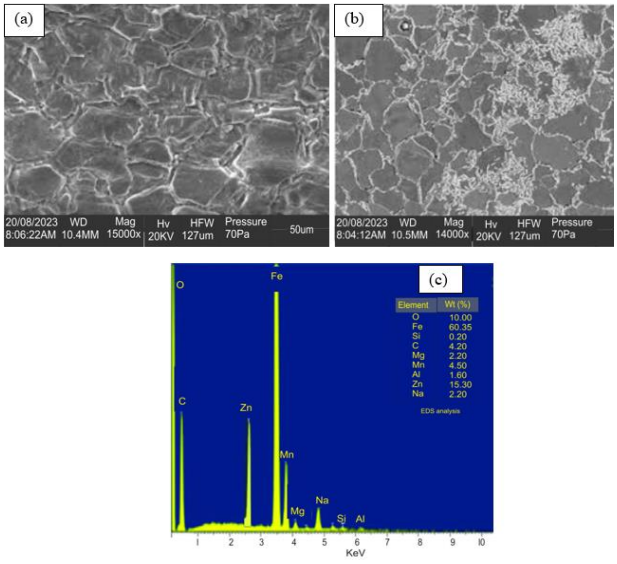

Fig. 5: Sample B SEM and EDX (a) uncorroded part (b) inside cor-roded part (c) EDX analysis of corroded part

4. Conclusion

The effect of coupling two dissimilar steel pipes for borehole application was investigated. From the result, it shows that the carbon content of the two steels was different. The optical microstructure shows the presence of ferrite and cementite in the microstructure of the pipes, with pipe A having more cementite than pipe B. The potential polarization shows steel pipe A has more negative potential and a high corrosion current than steel pipe B, which makes pipe A anode and pipe B cathode. The SEM/EDX analysis shows more corrosion on pipe A than on pipe B.

References

Bagheri, A.H., Nasrazadani, S. and Bostanci, H., 2017. Impact of Internal Pipe Grooves on Flow-Accelerated Corrosion of Small-Bore A-106 Carbon Steel Pipes. *Journal of Failure Analysis and Prevention*, *17*, pp.417-425.

Bellucci, F., 1991. Galvanic corrosion between nonmetallic composites and metals: I effect of metal and of temperature. *Corrosion*, *47*(10), pp.808-819.

Ghorbani, S., Ghasemi, R., Ebrahimi-Kahrizsangi, R. and Hojjati-Najafabadi, A., 2017. Effect of post weld heat treatment (PWHT) on the microstructure, mechanical properties, and corrosion resistance of dissimilar stainless steels. *Materials Science and Engineering: A*, *688*, pp.470-479.

Hasan, B.O., 2014. Galvanic corrosion of carbon steel–brass couple in chloride containing water and the effect of different parameters. *Journal of Petroleum Science and Engineering*, *124*, pp.137-145.

Pleshivtsev, V., Filippov, G., Pak, Y. and Livanova, O., 2009. Effect of carbon content and stressed state on the corrosion rate of pipe steel in heating systems. *Metallurgist*, *53*.

Satoh, T., Shao, Y., Cook, W.G., Lister, D.H. and Uchida, S., 2007. Flow-assisted corrosion of carbon steel under neutral water conditions. *Corrosion*, *63*(8), pp.770-780.

Shaik, L.A. and Thamida, S.K., 2019. Studies on galvanic corrosion of tri-metallic joint of steels in sodium chloride solution. *Materials Today: Proceedings*, *15*, pp.57-62.

Sun, F., Li, X. and Cheng, X., 2014. Effects of carbon content and microstructure on corrosion property of new developed steels in acidic salt solutions. *Acta Metallurgica Sinica (English Letters)*, *27*, pp.115-123.

Tavakkolizadeh, M. and Saadat manesh, H., 2001. Galvanic corrosion of carbon and steel in aggressive environments. *Journal of Composites for construction*, *5*(3), pp.200-210.

Wang, Z., Zhang, X., Yu, H., Liu, J., Cheng, L., Hu, S.E. and Wu, K., 2022. Effects of pearlite on corrosion initiation and propagation in weathering steels in marine environments. *Journal of Materials Science*, *57*(10), pp.6039-6055.

Wu, H., Luo, Y. and Zhou, G., 2023. The evolution of the corrosion mechanism of structural steel exposed to the urban industrial atmosphere for seven years. *Applied Sciences*, *13*(7), p.4500.

Wu, W., Hu, S. and Shen, J., 2015. Microstructure, mechanical properties and corrosion behavior of laser welded dissimilar joints between ferritic stainless steel and carbon steel. *Materials & Design (1980-2015)*, *65*, pp.855-861.

Zhou, Y., Qi, J. and Engelberg, D.L., 2021. On the application of bipolar electrochemistry for simulating galvanic corrosion behaviour of dissimilar stainless steels. *Electrochemistry Communications*, *126*, p.107023.